PCCP

Hierarchical Heterostructure of Ag-Nanoparticle Decorated Fullerene Nanorods (Ag-FNRs) as an Effective Single Particle Freestanding SERS Substrate

Journal:	*Physical Chemistry Chemical Physics*
Manuscript ID	CP-ART-05-2018-002779.R2
Article Type:	Paper
Date Submitted by the Author:	26-Jun-2018

Complete List of Authors:	Kumar, Gundam; Indian Association for the Cultivation of Science, Centre for Advanced Materials; Indian Association for the Cultivation of Science (IACS), Shrestha, Rekha; Tokyo University of Science, Department of Pure and Applied Chemistry, Faculty of Science and Technology Ji, Qingmin; Nanjing University of Science and Technology Hill, Jonathan; National Institute for Materials Science, Center for Materials Nanoarchitectonics Ariga, Katsuhiko; National Institute for Materials Science, World Premier International (WPI) Research Center for Materials Nanoarchitectonics (MANA) Acharya, Somobrata; Indian Association for the Cultivation of Science, Centre for Advanced Materials Shrestha, Lok Kumar; National Institute for Materials Science (NIMS), WPI Center for Materials Nanoarchitectonics (MANA)

Journal Name

ARTICLE

Hierarchical Heterostructure of Ag-Nanoparticle Decorated Fullerene Nanorods (Ag-FNRs) as an Effective Single Particle Freestanding SERS Substrate

Received 00th January 20xx,
Accepted 00th January 20xx

DOI: 10.1039/x0xx00000x

www.rsc.org/

Gundam Sandeep Kumar,[#,a] Rekha Goswami Shrestha,[#,b] Qingmin Ji,[c] Jonathan P. Hill,[c] Katsuhiko Ariga,[b,d] Somobrata Acharya*[a] and Lok Kumar Shrestha*[b]

A hierarchical heterostructure composed of silver nanoparticles (Ag-NPs: average diameter ~10 nm) on fullerene nanorods (FNRs: average length ~11 μm and average diameter ~200 nm) was fabricated using a simple solution route. It was used as an effective single particle freestanding surface enhanced Raman scattering (SERS) substrate for the detection of target molecules (Rhodamine 6G: R6G). FNRs were formed ultra-rapidly (formation process completed in a few seconds) at a liquid-liquid interface of methanol and C_{60}/mesitylene solution then Ag-NPs were grown directly on the surfaces of the FNRs by treatment with a solution of silver nitrate in ethanol. This unique hierarchical heterostructure allows efficient adsorption of target molecules also acting as an effective SERS substrate capable of detecting the adsorbed R6G molecules in the nanomolar concentration range. In this study, SERS spectra are acquired on an isolated single Ag–FNR for the detection of the absorbed molecule rather than from a bulk, large area film composed of silver/gold nanoparticles as used in conventional methods. Thus, this work provides a new approach for the design and fabrication of freestanding SERS substrates for molecular detection applications.

Introduction

Nanostructured materials synthesis through self-assembly of building blocks with molecular level precision enables the fabrication of novel functional systems with well-defined architectures through the emerging concept of materials nanoarchitectonics.[1-5] Buckyball fullerene C_{60}, which is regarded as an ideal zero-dimensional (0D) nano-object, can be assembled into various nanostructured materials of higher dimensionality by applying the materials nanoarchitectonics concept. These self-assembled nanostructured fullerene crystals display unique optoelectronic properties including high electron mobility, high photosensitivity, electron transport properties and excellent electron-accepting properties.[6-11] Fullerene (C_{60}), particularly in its self-assembled states has attracted a great deal of interest and it has been applied in various fields including organic solar cells, optical limiting devices, superconductors, organic thin film transistors and spintronics.[12-19] Therefore, studies on the fabrication of self-assembled fullerene nano- or microcrystals have been continuously growing in order to improve device performance. Of various material fabrication methods, the liquid-liquid interfacial precipitation (LLIP) method has become a versatile yet simple method to produce various well-defined nanostructures of different dimensionalities.[20-22] In the LLIP technique, fullerene crystal formation is driven by supersaturation caused by the low solubility of fullerene especially in alcohols (antisolvent). Differences in solubility of C_{60} in antisolvents and good solvents play a key role and affect the morphology of the resulting crystalline materials.

Low dimensional fullerene nanomaterials (nanorods or nanotubes) have been extensively studied in the past due to their promising applications in solar cells, batteries, fuel cells, sensors, catalysis, etc.[21-28] Aligned fullerene nanowhiskers have also been explored for biological applications and recent studies have shown that cells undergo oriented growth along the axis of alignment of the nanowhiskers.[29] Establishing control over the shapes and sizes of individual nanostructures (mono-component crystals) has allowed the exploitation of several new properties although combining these diverse functionalities within individual nanocrystals remains challenging. Alternatively, hetero-nanostructured materials or doped systems can be used to integrate any individual properties or might be used to generate additional interesting new properties, which can be used for multiple applications. One-dimensional semiconductor heterostructures and interfaces have become of particular interest as nanoscale building blocks for future optoelectronic and nano-electronic miniaturized devices, and remarkable efforts are

[a] Center for Advanced Materials (CAM), Indian Association for the Cultivation of Science (IACS), Jadavpur, Kolkata 700 032, India.
[b] International Center for Materials Nanoarchitectonics (WPI-MANA), National Institute for Materials Science (NIMS), 1-1 Namiki, Tsukuba 305-0044, Japan
[c] Herbert Gleiter Institute of Nanoscience, Nanjing University of Science & Technology, 200 Xiaolingwei, Nanjing 210094, China
[d] Department of Advanced Materials Science, Graduate School of Frontier Sciences, The University of Tokyo, 5-1-5 Kashiwanoha, Kashiwa, Chiba 277-8561, Japan
*Corresponding author: SHRESTHA.Lokkumar@nims.go.jp; camsa2@iacs.res.in
[#] G.S.K and R.G.S. have equally contributed to this work.
†Electronic Supplementary Information (ESI) available: Additional SEM, TEM and HR-TEM images, XPS O 1s spectra and additional SERS data. See DOI: 10.1039/x0xx00000x

currently being made for the synthesis and study of the electronic and optical properties of advanced nanowire heterostructures. Hybrid nanostructures of fullerenes, π–conjugated polymers and metal nanoparticles (NPs) represent a new class of nanomaterials in which organic and inorganic components are integrated but exhibiting unique properties. Also, fullerene–semiconductor nanocrystal composites such as P3HT-doped fullerene nanocrystals have been designed and employed for photovoltaic applications.[30, 31] There have been a number of recent reports that the power conversion efficiencies of photovoltaic devices based on π-conjugated polythiophene–fullerene composites are improved by incorporating plasmonically active metal NPs into the composites.[32,33] Recently, a hybrid structure of fullerene C_{60}-polythiophene nanotubes with metal NPs was developed for plasmonic studies by template-based electrocopolymerization of terthiophene-linked C_{60} and terthiophene modified silver or gold NPs.[32] In general, metal NPs, especially silver and gold, have proven to be excellent candidates for surface-enhanced Raman scattering (SERS), which is a very promising phenomenon for applications in molecular sensing applications. Most of these attractive applications are based on the localized surface plasmon resonances (LSPRs) of metal NPs due to the significant electromagnetic field enhancement near the metal surface. However, the effect of doping/functionalization or growing different nanostructured materials such as metal nanoparticles on the surface of fullerene nanowhiskers for the detection of molecules has not been well investigated to date.

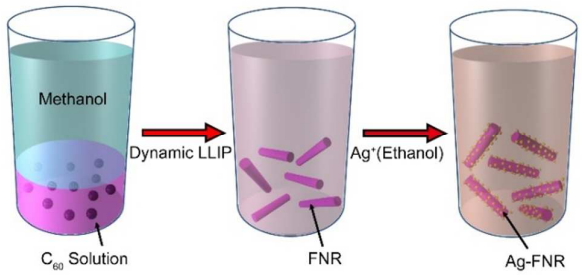

Scheme 1. Schematic representation of the reactions involved in the synthesis of FNR from a fullerene–mesitylene solution followed by the formation of Ag–FNRs heterostructures upon the addition of the $AgNO_3$–ethanol solution to the FNR.

In this contribution, we report a novel hierarchical heterostructure composed of fullerene nanorods (Ag–FNR) decorated with silver nanoparticles as an efficient surface enhanced Raman scattering (SERS) substrate for the detection of the fluorescent organic dye Rhodamine 6G (R6G) molecules at nanomolar (10^{-9} M) concentrations. This novel freestanding plasmonic Ag-FNR was prepared by a simple solution-based strategy (**Scheme 1**). First, fullerene C_{60} nanorods (FNRs) were prepared ultrarapidly under ambient conditions at a liquid-liquid interface between methanol and a saturated solution of C_{60} in methanol.[21] A solution of silver nitrate in ethanol was then added to the FNRs followed by gentle hand shaking for 4 – 5 min. The mixture was then stored in a dark place for 48 h for the growth of hierarchical Ag–FNR heteronanostructure. Ag–NPs (average size ~ 10 nm) were observed to have uniformly and homogeneously formed at the surfaces of the FNRs. As prepared individual isolated hierarchical Ag–FNR heterostructure was employed as an efficient SERS substrate for the detection of R6G molecules. We have found that Ag–FNR free standing SERS substrate is capable of detecting adsorbed molecules even at nanomolar concentrations.

Experimental Section

Materials

Pristine fullerene C_{60} (pC_{60}) powder of purity >99.5% was obtained from Materials Technologies Research, Ltd. (Cleveland, OH). Methanol and mesitylene of purity >99% were purchased from the Wako Chemical Corporation, Japan. Silver nitrate ($AgNO_3$) salt was purchased from Tokyo Chemical Industry, Tokyo, Japan. All chemicals were used as received.

Synthesis of FNRs.

FNRs were prepared using methanol and mesitylene respectively as antisolvent and solvent for C_{60} following the LLIP method reported in our previous work.[21]

Synthesis of Ag-FNR heterostructure.

For the synthesis of Ag–FNR, as-prepared FNRs were washed with fresh ethanol solution 4–5 times by repeated centrifugation (6,000 rpm) to remove mesitylene and methanol from the FNRs suspension. FNRs were then dispersed into a freshly prepared ethanol solution of $AgNO_3$ (2 mL: 100 mM) by gentle hand shaking for 4–5 min. The mixture was then stored in a dark place for 48 h for the growth of hierarchical Ag–FNR heteronanostructure. Finally, the Ag–FNR was then washed with ethanol, separated by centrifugation and this material was used for characterizations and further studies.

Characterizations.

FNRs and Ag–FNR were characterized by scanning electron microscopy (SEM: S-4800, Hitachi Co. Ltd., Japan, operated at 10 kV), transmission electron microscopy (TEM: JEOL Model JEM-2100F, operating at 200 kV), energy dispersive X-ray spectroscopy (EDS) and X-ray photoelectron spectroscopy (XPS: Thermo Electron Co., Germany).

Surface Enhanced Raman Scattering (SERS) study.

The Raman spectrometer (Jobin-Yvon T64000) was wavelength-calibrated using a silicon wafer, focused and collected as a static spectrum centered at 521 cm^{-1}. Visible SERS spectra were recorded using a Horiba/Jobin Yvon laser Raman analyzer LabRAM HR 800 (Horiba/Jobin Yvon, JAPAN) equipped with a frequency doubled Nd:YAG 514 nm laser. Samples were excited using green laser (514.5 nm, 0.025 mW power). A suspension of Ag-FNR heterostructures (50 μL) was directly drop-coated onto a piece of clean dry silicon wafer then R6G solution (10 μL) was drop cast on the as-prepared Ag-FNR film followed by drying at reduced pressure for 6 h. The concentration of the R6G solution was varied between 0.1 nM and 1 μM for the SERS study.

Results and Discussion

Ultrarapid formation of self-assembled C_{60} crystals at the interface between methanol and a mesitylene solution saturated with C_{60} yielded FNRs with a uniformly distributed 1D crystalline morphology

(**Figure 1a, b**). Their linear rodlike morphology, faceted structures and hexagonal cross-sections can be seen in the high-resolution SEM images (Electronic Supporting Information: **Figure S1**). SEM observations revealed the pristine appearance of the surfaces of the FNRs with lengths lying in the range 2–25 μm (average around ~ 11 μm) and mean diameter of ~215 nm. Histograms of length and diameter distributions of FNRs are shown in **Figure S1e** and **S1f**, respectively. Although the diameter of FNRs varies from 80 – 450 nm, the diameters of individual FNRs are uniform along their entire lengths demonstrating the uniform growth of the rods. Ultrarapidly formed FNRs are quite reproducible. Similar structure, morphology and distributions (length and diameter) are observed over several batches of synthesis. The highly crystalline nature of these FNRs was confirmed by TEM observations (**Figure S2**). Spot type SAED pattern (**Figure 2a**) and extended lattice fringes of C_{60} with lattice spacing of 1.02 nm (corresponding to the distance between 110 planes of hexagonal close pack structure) can be seen in HR-TEM images (**Figure 2b**). Additional TEM and HR-TEM images of FNRs are supplied in **Figure S2**. XRD pattern of ultra-rapidly formed FNR corresponds to the hexagonal close-pack (*hcp*) crystal structure while, pristine C_{60} display face-centered cubic (*fcc*) structure with cell dimension ca. a = 1.240 nm.[21] The cell dimensions of FNR were ca. a = 2.401 nm, c = 1.025 nm (a/c = 2.342), which are similar to the *hcp* structures of previously reported C_{60} solid solvates and could be indexed to $P6_3$ space group with solvent molecules between layers with a 3-fold symmetry near the 6_3 screw axis.

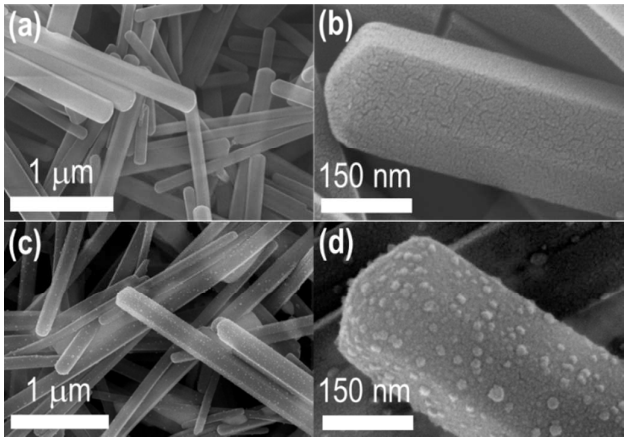

Fig. 1 (a) SEM image of 1D FNR synthesized by the LLIP method at the interface between methanol and a saturated solution of C_{60} in mesitylene at 25 °C, (b) high resolution SEM image highlighting the clean-faceted surfaces, (c) SEM image of the Ag–FNR heterostructure and (d) corresponding high resolution SEM image revealing well distributed uniformly dimensioned Ag–NPs on the surfaces of the FNRs.

Addition of the $AgNO_3$-ethanol into the FNR suspension followed by aging for 48 h in the dark resulted in formation of hierarchical Ag–FNR heteronanostructure (**Figure 1c, d**). Ag-coated FNRs were prepared by the spontaneous electron transfer from C_{60} to Ag ion. Due to the electron transfer, C_{60} is oxidised and Ag nanoparticles are formed. Similar spontaneous electron transfer from C_{60} to Au ions, i.e. oxidation of C_{60} and hole doping, has been observed resulting in the formation of Au-coated C_{60} nanowires.[34,35]

A uniform distribution of Ag–NPs on each facet of the FNRs can be observed in higher resolution SEM images (**Figure 1d** and **Figure S3d-h**). The histogram based on particle diameters suggests a mean diameter of ~ 12 nm Ag–NPs (**Figure S4**). Low magnification SEM images reveal that dimensions (length and diameter) of the FNRs does not vary after formation of Ag–FNR heteronanostructure (**Figure 1a** and **Figure S3a-c**), which indicates that the Ag–NPs formation process does not have any impact on the morphology of the FNRs.

As confirmed by SEM observation, TEM images also reveal the solid morphology of FNRs with nanosized Ag-NPs uniformly distributed on their surfaces (**Figure 2c** and **Figure S5**). Uniform decoration of Ag-NP on the surface of FNRs can also be seen in dark-field TEM images (**Figure S6a, b**). HR-TEM images show the densely packed lattice planes of both fullerene C_{60} and silver (**Figure 2d** and **Figure S6c-f**). Furthermore, HR-TEM clearly reveals the attachment of the Ag-NPs to the surface of the FNRs, i.e. Ag–FNR is a heteronanostructure.

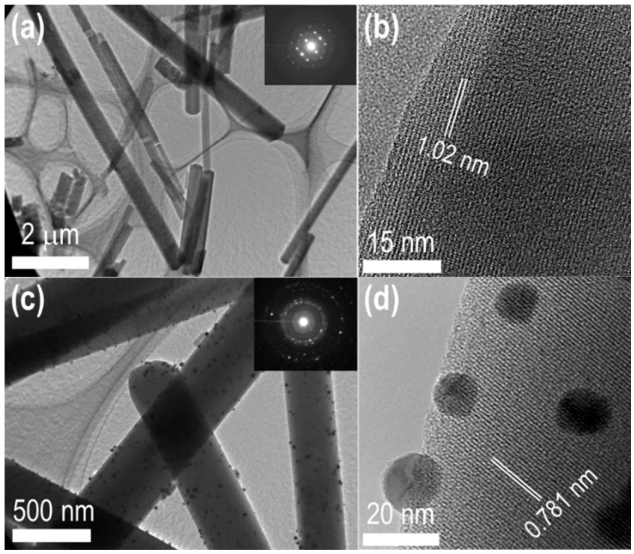

Fig. 2 (a) TEM image of ultrarapidly formed FNRs, (b) HR-TEM images from the thinnest area of a single FNR indicates the high crystallinity, (c) TEM image of the Ag–FNRs heterostructures displaying the rod morphology with Ag–NPs attached at the surfaces of the FNRs and (d) HR-TEM image of the Ag–FNR. Inset of panels (a) and (c) corresponds to the SAED pattern.

Using TEM/EDS elemental mapping (**Figure 3**) distribution of Ag–NPs on the FNRs was further studied. TEM/EDS analyses reveals the uniform distribution of Ag–NPs on the surface of the FNR, which is obvious from the dark field TEM image (**Figure 3a**). Elemental mapping images confirm the presence of constituent elements carbon (C) and silver (Ag). **Figure 3b** clearly shows a uniform distribution of carbon due to the fullerene nanocrystals and confirms that the nanorods are composed of the fullerene self-assembly. **Figure 3c** shows the presence of Ag-nanoparticles uniformly distributed on the surfaces of the FNRs. The uniform distribution of carbon and silver can also be seen in the combined elemental map (**Figure 3d**).

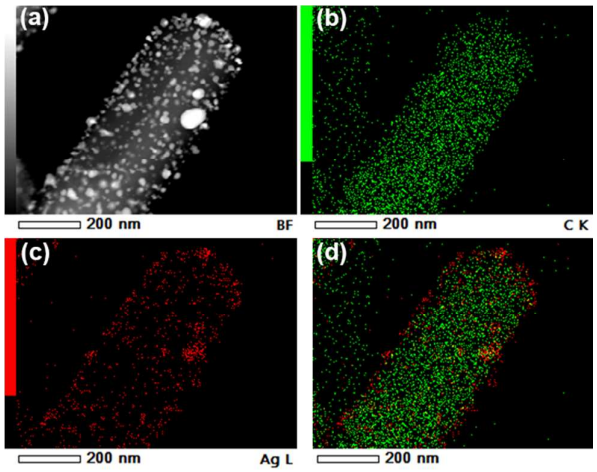

Fig. 3 TEM/EDS elemental analysis of an Ag–FNR revealing the presence of carbon and silver; (a) STEM image (b), elemental mapping of carbon, (c) silver, and (d) combined carbon and silver.

Surface composition of the Ag–FNRs was further characterized by XPS (**Figure 4**). The XPS survey spectrum clearly shows the presence of carbon, silver and oxygen and a trace of nitrogen (Figure 4a). Two characteristic peaks corresponding to $3d_{5/2}$ and Ag $3d_{3/2}$ can be found in the Ag 3d spectrum due to metallic Ag (**Figure 4b**). These peaks were deconvoluted into four components (each peak into two components). For the Ag $3d_{3/2}$ spectrum, the major peak (373.8 eV) accounts for 34.3 atom%, while the minor peak (373.2 eV) accounts for 5.9 atom% while the Ag $3d_{5/2}$ peak contains a major component peak (367.7 eV) for 50.1 atom% and a minor peak (368.2 eV) accounting for 9.7 %. Binding energy of Ag $3d_{5/2}$ ca. 367.7 eV with 6.1 eV peak splitting of the 3d doublet confirms that the silver species exists as Ag(0) at the surface of the FNRs. Deconvolution of C 1s spectra of pC_{60}, FNR and Ag–FNR confirm C=C (sp^2), C–C (sp^3) and O–C=O or C–O bonding states (**Figure 4c**). Note that the C 1s peak centered at 283.7 eV in the Ag–FNR sample corresponds to a metal-carbon bond (as indicated by M–C in Figure 4c). Deconvoluted XPS O 1s spectra of pC_{60}, FNR and Ag–FNR are shown in **Figure S7**.

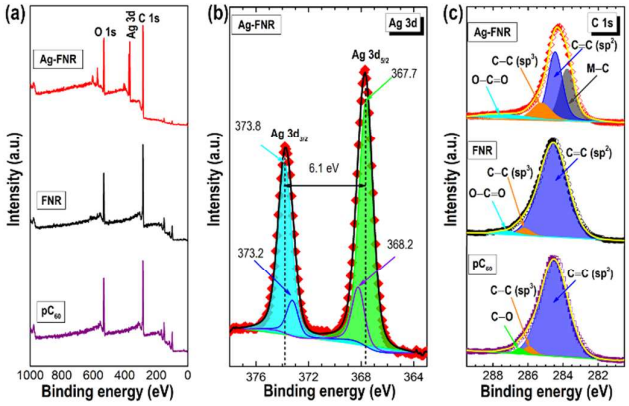

Fig. 4 (a) XPS survey spectra of pC_{60}, FNR and Ag–FNRs, (b) XPS Ag 3d spectra including deconvolution and (c) XPS C 1s spectra including deconvolution for pC_{60}, FNR and Ag–FNRs.

The SERS technique yields greatly enhanced Raman signals from Raman-active molecules that have been adsorbed at a specially prepared metal surface. SERS uses photons as a probe and results in high-sensitivity and high-resolution spectra without causing damage to the analyte samples, and provides detailed information regarding interactions between adsorbates and substrates. Raman signals are typically very weak although when molecules are adsorbed onto roughened surfaces or nanoparticles composed of Ag or Au, Raman signals can be significantly enhanced (i.e. SERS effect). This phenomenon has consequently been widely explored for applications related to single molecule detection. Conventionally, the SERS effect has been studied by depositing an analyte or target molecule on a rough metal surface or some metal nanostructure. However, to date, SERS effects on freestanding nanorods or nanotubes incorporating metal NPs had not been well explored. Based on the potential of metal-decorated freestanding nanorods, we have studied the SERS properties of our newly-synthesized Ag–NPs-decorated FNRs (Ag–FNR). Silver nanoparticles were formed on the surfaces of the ultra-rapidly formed FNRs and the resulting freestanding Ag–FNRs were employed as a SERS substrate for R6G molecular detection up to the nanomolar level. Silver nanoparticles decorated on the FNRs surfaces play an important role in magnifying the surface local electric field in the vicinities of the silver nanostructures through resonant surface plasmon excitation.

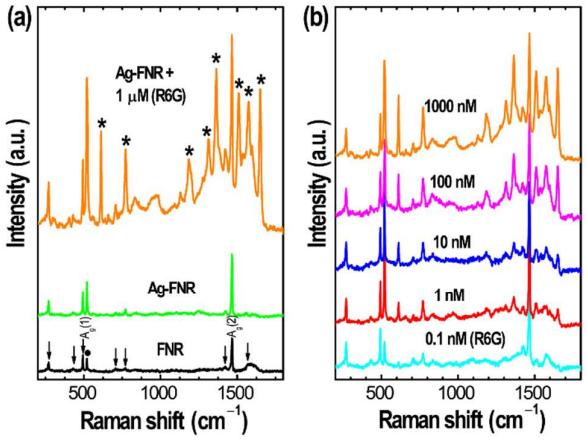

Fig. 5 (a) Raman spectra of pC_{60}, FNR, Ag-FNR and 1 μM R6G analyte adsorbed onto the Ag-FNR as typical example, (b) Raman spectra (SERS) collected from the Ag-FNR with different concentration of R6G (0.1, 1, 10, 100 and 1000 nM). Arrows in panel (a: for pC_{60}) indicate six vibrations H_g modes of C_{60} and the "●" symbol indicates the Raman band originating from the silicon substrate and "*" symbol indicates the SERS signal from R6G molecules adsorbed on the Ag-FNR substrate.

The Raman scattering spectrum acquired from bare FNRs deposited on a silicon substrate contains peaks at 273, 432, 496, 710, 772, 1424, 1465, and 1575 cm^{-1}, which are very similar to the Raman bands of pC_{60} (highlighted by arrows in **Figure 5a**). These bands correspond to two A_g ($A_g(1)$ at 496 cm^{-1}, for the breathing mode and $A_g(2)$ at 1465 cm^{-1} for the pentagonal pinch mode) and six H_g vibration modes ($H_g(1)$ at 273 cm^{-1}, $H_g(2)$ at 432 cm^{-1}, $H_g(4)$ at 710 cm^{-1}, $H_g(5)$ at 772 cm^{-1}, $H_g(6)$ at 1424 cm^{-1} and $H_g(8)$ at 1575 cm^{-1}). The positions of Raman bands remain essentially unchanged in FNRs, demonstrating that molecular C_{60} dominates and their

molecular rotation/vibrations are apparently unaffected in the FNR, i.e. FNR is purely a van der Waals solid. Polymerization of fullerene molecules was not observed following laser beam irradiation during Raman measurements. The Raman spectrum acquired from Ag–FNRs deposited on a silicon substrate exhibited Raman peaks similar to FNR with some additional and split modes resulted from the symmetry lowering and selection rule relaxation caused by Ag–NP attachment at the surfaces of FNRs (**Figure 5a**). The additional and split modes were also clearly detected due to the SERS effect in Ag–FNR with 1 μM R6G.

It is well known that the greatest SERS enhancement is expected when extremely high local electric fields are generated by excitation of the surface plasmon. In the present study, we have employed Ag-FNRs as an effective freestanding substrate for the detection of R6G molecules absorbed at its surfaces. Ag nanoparticles in the Ag-FNR heterostructure create hot sites for the enhancement of SERS signals. For the preparation of SERS substrate, a suspension of Ag–FNR was drop cast onto a silicon substrate and dried under reduced pressure for 6 h. Aliquots of aqueous solutions of the target molecule R6G (10 μL) at different concentrations (0.1, 1, 10, 100 and 1000 nM) were then added to the Ag–FNR film and it was dried under reduced pressure for 6 h. Raman spectra acquired from the R6G adsorbed Ag–FNR displayed reliable Raman signals at ~ 613, 774, 1124, 1183, 1311, 1363, 1511, 1575 and 1649 cm^{-1} corresponding to the R6G molecules. The vibrational bands of the R6G dye lie in the range 600 to 1700 cm^{-1}. Vibrational bands observed in the R6G spectra can be assigned as follows: ~ 613 cm^{-1} is due to C–C–C in-plane bending vibrations, 774 cm^{-1} arises from C–H out-of-plane bending vibrations, 1124 cm^{-1} and 1183 cm^{-1} arise from C–H in-plane bending vibrations, with remaining bands in the 1311–1649 cm^{-1} range being due to aromatic C–C stretching vibrations.[36, 37] In general, continuous films of rough metal surfaces are used as SERS substrates.[38] Furthermore, assembled metal nanostructures into hierarchical structures have also been used as effective SERS substrates for the molecular detection.[37-39] However, here we have used freestanding Ag–FNR nanostructures as an effective SERS substrate for molecule detection (**Figure S8**: Optical micrographs before and after Raman laser irradiation). Ag–FNRs show significant enhancement in the Raman signals of the analyte adsorbed at its surface. In contrast, no obvious Raman peaks of R6G were observed on FNR-only substrate under the same conditions. The signal enhancement observed above suggests that the presence of Ag–NPs acts like hot spots for the localized surface plasmon on the FNR structure and enhances the SERS signal of the R6G analyte present on the surface of the Ag–FNR free standing substrate. The SERS enhancement factor (EF) calculated by following the reported method.[42] The EF for different peaks located at 613, 774, 1363, 1511, 1577, 1649 cm^{-1} (at 10^{-6} M of R6G) found to be 2.41 x 10^5, 2.31 x 10^5, 2.73 x 10^5, 2.57 x 10^5, 2.62 x 10^5, respectively from Ag-FNR SERS substrates. Two peaks centered at 613 and 1183 cm^{-1} are clearly seen in the spectra for all concentrations of R6G up to 1 nM. These Raman bands showed monotonous decay of the SERS intensity upon decreasing concentration of R6G (**Figure S9**). In a control experiment Ag nanoparticle thin film prepared on a planar substrate was used as the SERS substrate and SERS signal was recorded for R6G (1 μM). The SERS signal enhancement of Ag-FNRs is more clear and convincing (**Figure S10**). From the above experimental observations, it is very obvious that the novel hierarchical Ag–FNRs heterostructure can indeed serve as robust SERS substrate for the detection of R6G at nanomolar concentrations.

Conclusions

In conclusion, we have demonstrated a simple solution-based approach for the fabrication of hierarchical heterostructures of Ag-nanoparticles on fullerene nanorods (Ag–FNRs), which functions as an effective SERS substrate for the detection of Rhodamine 6G molecules in the nanomolar concentration range. Initially, we prepared FNRs at the liquid-liquid interface between methanol and a solution of fullerene C_{60} in mesitylene. Ag-NPs were then grown directly (in-situ method) on the surface of the FNRs by addition of a solution of $AgNO_3$ in ethanol. Aging this solution leads to the nucleation and growth of Ag nanoparticles on the surfaces of the FNRs. Ag–NPs were grown and distributed uniformly on the surface of the FNRs. This plasmonically active Ag–FNRs substrate could be used for effective SERS detection of standard Rhodamine 6G molecules at a concentration of ~10^{-9} M. SERS performance was studied by applying confocal Raman imaging on the individual isolated Ag–FNR in contrast to the conventional continuous SERS films, which are formed from inhomogeneous metallic surfaces. The approach developed and demonstrated here opens up new possibilities for the preparation of efficient freestanding plasmonic substrates for application in molecular detection.

Acknowledgements

This work was partially supported by JSPS KAKENHI (Coordination Asymmetry) (Grant No. JP16H06518), and CREST JST (Grant No. JPMJCR1665). Authors thank Dr. Tadaaki Nagao, International Center for Materials Nanoarchitectonics (WPI-MANA) of National Institute for Materials Science (NIMS) for the fruitful discussion. GSK thanks the DST INSPIRE Program for Fellowship. SA acknowledges the financial support from DST, India.

Notes and references

1 L. Grill, M. Dyer, L. Lafferentz, M. Persson, M. V. Peters and S. Hecht, *Nat. Nanotechnol.*, 2007, **2**, 687-691.
2 S. C. Glotzer and M. J. Solomon, *Nat. Mater.*, 2007, **6**, 557-562.
3 L. Zang, Y. Che and J. S. Moore, *Acc. Chem. Res.*, 2008, **41**, 1596-1608.
4 L. K. Shrestha, Q. Ji, T. Mori, K. Miyazawa, Y. Yamauchi, J. P. Hill and K. Ariga, *Chem. Asian J.*, 2013, **8**, 1662-1679.
5 L. K. Shrestha, R. G. Shrestha, J. P. Hill and K. Ariga, *J. Oleo. Sci.*, 2013, **62**, 541-553.
6 H. Li, B. C. K. Tee, J. J. Cha, Y. Cui, J. W. Chung, S. Y. Lee and Z. Bao, *J. Am. Chem. Soc.*, 2012, **134**, 2760-2765.
7 K. Itaka, M. Yamashiro, J. Yamaguchi, M. Haemori, S. Yaginuma, Y. Matsumoto, M. Kondo and H. Koinuma, *Adv. Mater.*, 2006, **18**, 1713-1716.
8 J. D. Zimmerman, V. V. Diev, K. Hanson, R. R. Lunt, E. K. Yu, M. E. Thompson and S. R. Forrest, *Adv. Mater.*, 2010, **22**, 2780-2783.

9 H.-X. Ji, J.-S. Hu, L.-J. Wan, Q.-X. Tang and W.-P. Hu, *J. Mater. Chem.*, 2008, **18**, 328-332.
10 M. Thomas, B. J. Worfolk, D. A. Rider, M. T. Taschuk, J. M. Buriak and M. J. Brett, *ACS Appl. Mater. Interfaces*, 2011, **3**, 1887-1894.
11 V. S. Nair, R. D. Mukhopadhyay, A. Saeki, S. Seki and A. Ajayaghosh, *Sci. Adv.*, 2016, **2**, 1600142.
12 R. Ahmed, A. Kadashchuk, C. Simbrunner, G. Schwabegger, M. Havlicek, E. Głowacki, N. S. Sariciftci, M. A. Baig and H. Sitter, *Org. Electron.,* 2014, **15**, 175-181.
13 S. Collavini, M. Saliba, W. R. Tress, P. J. Holzhey, S. F. Völker, K. Domanski, S. H. Turren-Cruz, A. Ummadisingu, S. M. Zakeeruddin, A. Hagfeldt, M. Grätzel and J. L. Delgado, *ChemSusChem*, 2018, **11**, 1-9.
14 C. Zhang, A. Mumyatov, S. Langner, J. D. Perea, T. Kassar, J. Min, L. Ke, H. Chen, K. L. Gerasimov, D. V. Anokhin, D. A. Ivanov, T. Ameri, A. Osvet, D. K. Susarova, T. Unruh, N. Li, P. Troshin and C. J. Brabec, *Adv. Energy. Mater.*, 2017, **7**, 1601204.
15 H. Takeya, K. Miyazawa, R. Kato, T. Wakahara, T. Ozaki, H. Okazaki, T. Yamaguchi and Y. Takano, *Molecules*, 2012, **17**, 4851-4859.
16 J. Guan and D. Tománek, *Nano Lett.,* 2017, **17**, 3402-3408.
17 F. Huang, Y. Li, H. Xia, J. Zhang, K. Xu, Y. Peng and G. Liu, *Carbon*, 2017*,* **118***,* 666-674.
18 Q. Burlingame, C. Coburn, X. Che, A. Panda, Y. Qu and S. R. Forrest, *Nature*, 2018, **554**, 77-80.
19 H. Liu, J. Wang, M. Groesbeck, X. Pan, C. Zhang and Z. V. Vardeny, *J. Mater. Chem. C*, 2018, **6**, 3621-3627.
20 L. K. Shrestha, J. P. Hill, T. Tsuruoka, K. Miyazawa and K. Ariga, *Langmuir*, 2013, **29**, 7195-7202.
21 R. G. Shrestha, L. K. Shrestha, A. H. Khan, G. S. Kumar, S. Acharya and K. Ariga, *ACS Appl. Mater. Interfaces*, 2014, **6**, 15597-15603.
22 K. Miyazawa, *Sci. Technol. Adv. Mater.*, 2015, **16**, 013502.
23 L. K. Shrestha, R. G. Shrestha, Y. Yamauchi, J. P. Hill, T. Nishimura, K. Miyazawa, T. Kawai, S. Okada, K. Wakabayashi and K. Ariga, *Angew. Chem. Int. Ed.*, 2014, **53**, 1-6.
24 P. Bairi, R. G. Shrestha, J. P. Hill, T. Nishimura, K. Ariga and L. K. Shrestha, *J. Mater. Chem. A*, 2016, **4**, 13899-13906.
25 S. S. Narwade, B. B. Mulik, S. M. Mali and B. R. Sathe, *Appl. Surf. Sci.,* 2017, **396**, 939-944.
26 N. Zhang, Y. Zhang, M.-Q. Yang, Z.-R. Tang and A. Xu, *J. Catal.*, 2013, **299**, 210-221.
27 S. Sutradhar and A. Patnaik, *Sens. Actuators B*, 2017, **241**, 681-689.
28 B. B. Prasad, R. Singh and A. Kumar, *Biosens. Bioelectron.*, 2017, **94**, 115-123.
29 V. Krishnan, Y. Kasuya, Q. Ji, M. Sathish, L. K. Shrestha, S. Ishihara, K. Minami, H. Morita, T. Yamazaki, N. Hanagata, K. Miyazawa, S. Acharya, W. Nakanishi, J. P. Hill and K. Ariga, *ACS Appl. Mater. Interfaces*, 2015, **7**, 15667-15673.
30 R. Saran, V. Stolojan and R. J. Curry, *Sci. Rep.*, 2014, **4**, 5041.
31 P. Brown and P. V. Kamat, *J. Am. Chem. Soc.*, 2008, **130**, 8890-8891.
32 R. Yoshida, T. Matsumura, T. Nakahodo and H. Fujihara, *Chem. Commun.*, 2014, **50**, 15183-15186.
33 L. Lu, Z. Luo, T. Xu and L. Yu, *Nano Lett.*, 2013, **13**, 59-64.
34 H. S. Shin, H. Lim, H. J. Song, H.-J. Shin, S.-M. Park and H. C. Choi, *J. Mater. Chem.*, 2010, **20**, 7183.
35 J. Yang, H. Lim, H. C. Choi and H. S. Shin, *Chem. Commun.*, 2010, **46**, 2575.
36 E. Kirubha and P. K. Palanisamy, *Adv. Nat. Sci.: Nanosci. Nanotechnol.* 2014, **5**, 045006.
37 A. N. Severyukhina, B. V. Parakhonskiy, E. S. Prikhozhdenko, D. A. Gorin, G. B. Sukhorukov, H. Möhwald and A. M. Yashchenok, *ACS Appl. Mater. Interfaces,* 2015, **7**, 15466-15473.
38 N. H. Kim, W. Hwang, K. Baek, Md. R. Rohman, J. Kim, H. W. Kim, J. Mun, S. Y. Lee, G. Yun, J. Murray, J. W. Ha, J. Rho, M. Moskovits and K. Kim, *J. Am. Chem. Soc.,* 2018, **140**, 4705-4711.
39 C. Zhu, G. Meng, Q. Huang, Z. Zhang, Q. Xu, G. Liu, Z. Huanga and Z. Chua, *Chem. Commun*., 2011, **47**, 2709–2711.
40 C. Zhu, G. Meng, Q. Huang, Z. Li, Z. Huang, M. Wang and J. Yuan, *J. Mater. Chem*., 2012, **22**, 2271.
41 M. J. Mulvihill, X. Y. Ling, J. Henzie and P. Yang, *J. Am. Chem. Soc.,* 2010, **132**, 268–274.
42 C. Zhu, G. Meng, P. Zheng, Q. Huang, Z. Li, X. Hu, X Wang, Z. Huang, Fa. Li and N. Wu, *Adv. Mater.*, 2016, **28**, 4871–4876.

Table of content

Hierarchical Heterostructure of Ag-Nanoparticle Decorated Fullerene Nanorods (Ag-FNRs) as an Effective Single Particle Freestanding SERS Substrate

Gundam Sandeep Kumar,[#,a] Rekha Goswami Shrestha,[#,b] Qingmin Ji,[c] Jonathan P. Hill,[c] Katsuhiko Ariga,[b,d] Somobrata Acharya*[a] and Lok Kumar Shrestha*[b]

A hierarchical heterostructure composed of silver nanoparticles on fullerene nanorods fabricated using a simple solution route functions as an effective single particle freestanding SERS substrate for the detection of target molecules (Rhodamine 6G: R6G) in nanomolar concentration range.